

## **ENVIRONMENTAL SIMULATION OF TUNNEL FIRES BY COMPUTATIONAL FLUID DYNAMICS\***

**JOJO S. M. LI**

**W. K. CHOW**

*The Hong Kong Polytechnic University, China*

### **ABSTRACT**

How computational fluid dynamics (CFD) is applied to predict the probable environment in a tunnel due to an accidental fire will be discussed in this article. Results on the fire-induced air flow and temperature distributions are useful for design purposes. Predicted results by CFD are compared with experimental data measured from full-scale burning tests. Changes of tunnel environment due to wind velocity, heat release rate of the fire, and thermal stratification effect are included. The limitations on solving the key equations numerically will also be outlined.

### **1. INTRODUCTION**

Computational Fluid Dynamics (CFD) techniques (or fire field models) are now accepted by professionals dealing with tunnel ventilation as a design tool to simulate the fire environment in tunnels. Some of those field models [e.g., 1-5] have been evaluated for simulating smoke movement in building fires. Simulating the probable tunnel environment under an accidental fire is not quite the same as that in a normal building because of the large aspect ratio of length to height, leading to differences in smoke dynamics. CFD is believed to be a technique suitable for studying the environmental conditions in a tunnel fire.

\*This project is funded by PolyU grant number G-V644.

When an object is burned, an uprising hot plume is created. Upon reaching the ceiling, it will spread radially along the horizontal direction as a ceiling jet. This differs from the case of a normal building, where a stable smoke layer might be formed rapidly because of the vertical barriers. In a tunnel, the ceiling jet would travel horizontally for quite a long distance from the fire, presenting an environment quite different from that in a normal building. This phenomenon can be simulated by CFD as noted.

In this article, experimental data by Apte, Green, and Kent [6] on pool fires in a ventilated tunnel will be used for comparison with CFD predictions made using the software PHOENICS 3.2 [7]. Limitations of the technique for practical design of safety and environmental systems will be outlined.

## 2. NUMERICAL SIMULATIONS

Following the experimental tunnel arrangement [6], the computational geometry of the tunnel is 90 m long, 5.4 m wide, and 2.4 m high as shown in Figure 1. A fuel pool fire of octane with heat of combustion of  $44.4 \text{ MJkg}^{-1}$  [8] was located 40 m down the tunnel. In studying the thermal balance in the heptane pool fire in road tunnels, it was suggested that [9-13] the external radiation fraction was about 20% to 40%, depending on the pool fire diameter. Taking into account radiation losses at the walls of the tunnel and incomplete combustion due to soot formation, the enthalpy of reaction used in this simulation was adjusted to  $30 \text{ MJkg}^{-1}$  [14]. The circular pool of 1 m diameter used in the experiments was modeled as a square pool with a similar area. The parameters in the CFD software for simulating tunnel pool fire are shown in Table 1. Three different air speeds of up to  $2 \text{ ms}^{-1}$  upstream of the fire were used. The fuel inflow rate and air speed measured in the experiments and the equivalent heat release rate used in the simulations are given in Table 2. The fire was represented by a thermal object with constant heat release rate without any changes upon operating the ventilation system.

A mesh system of 93 cells in the x-direction, 17 cells in the y-direction, and eight cells in the z-direction, giving 12648 cells total, was used for all the cases. The grids are uniformly distributed in the transverse direction, but not in the longitudinal. Finer grid sizes were used in the region close to the fire. The simulations were run in steady-state mode with 100 iterations to achieve convergence.

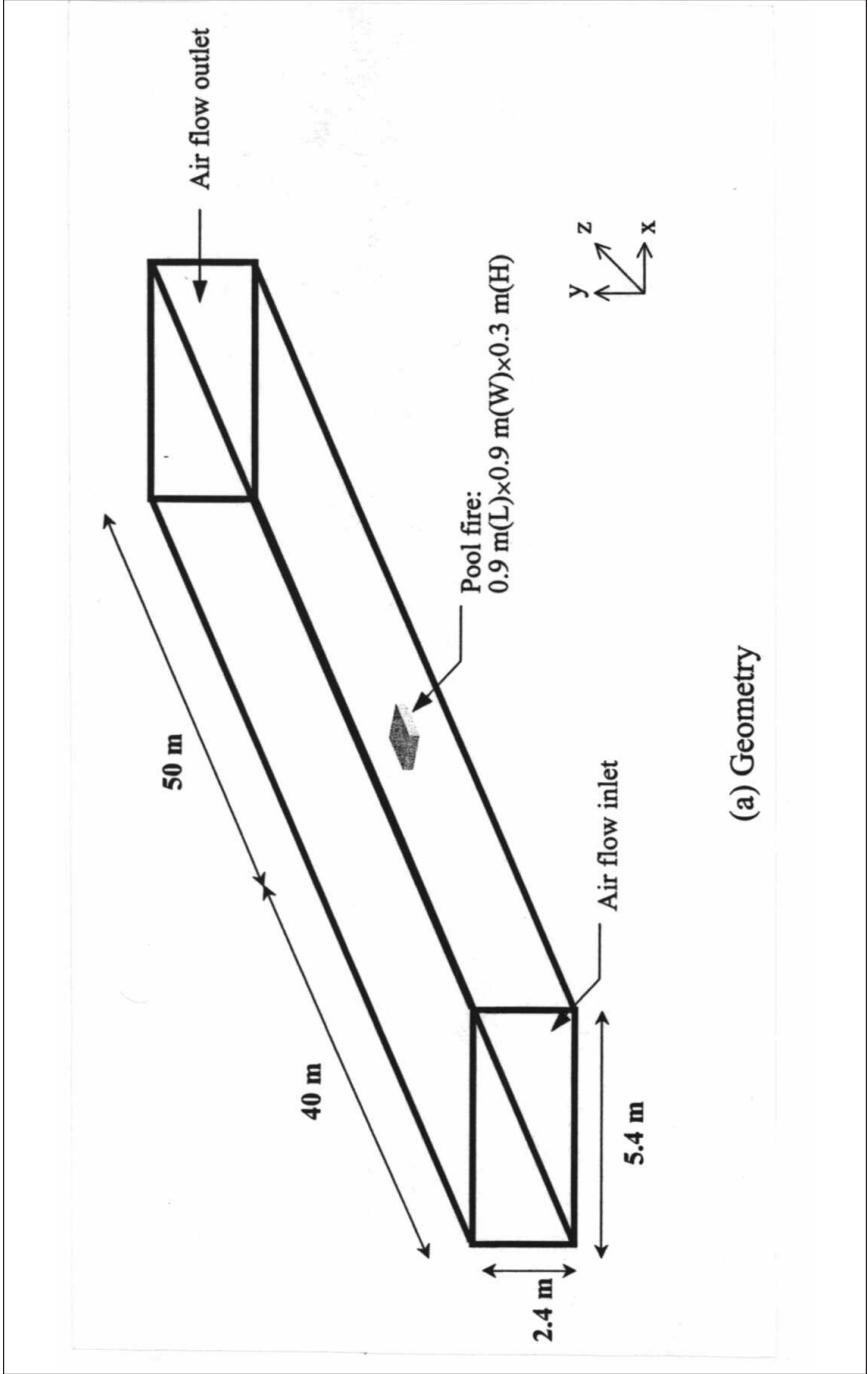
## 3. COMPARISON OF TUNNEL POOL FIRE MODELING AND EXPERIMENTAL RESULTS

The predicted vertical temperatures with and without radiation losses along the axis of the tunnel at various distances downstream of the fire are plotted in Figures 2 and 3.

Time dependence	Steady					
Gravitational forces	On					
Buoyancy model	Density difference					
Gravitational acceleration	X = 0	Y = -9.81 ms <sup>-2</sup>	Z = 0			
Reference density	1.189 kgm <sup>-3</sup>					
Coefficient for auto wall functions	Log-law					
Global wall roughness	0					
Turbulence model	k-ε					
Radiation model	Off					
Combustion model	Volumetric heat source					
Domain material	Air using Ideal Gas Law					
Reference pressure	1 × 10 <sup>5</sup> Pa					
Reference temperature	273 K					
Initial values	U = 0 ms <sup>-1</sup>	V = 0 ms <sup>-1</sup>	W = 0 ms <sup>-1</sup>	Differential pressure = 0, Pa	T = 293 K	KE = 0.01 m <sup>2</sup> s <sup>-2</sup>

Table 2. Simulation Conditions of Tunnel Pool Fire Experiments

Case	Fuel release rate (kgs <sup>-1</sup> m <sup>-1</sup> )	Air flow speed (ms <sup>-1</sup> )	Heat release rate without taking account of radiation losses (MW)	Heat release rate taking account of radiation losses (MW)
A	0.07	0.5	2.44	1.65
B	0.065	0.85	2.27	1.53
C	0.058	2	2.02	1.36



(a) Geometry

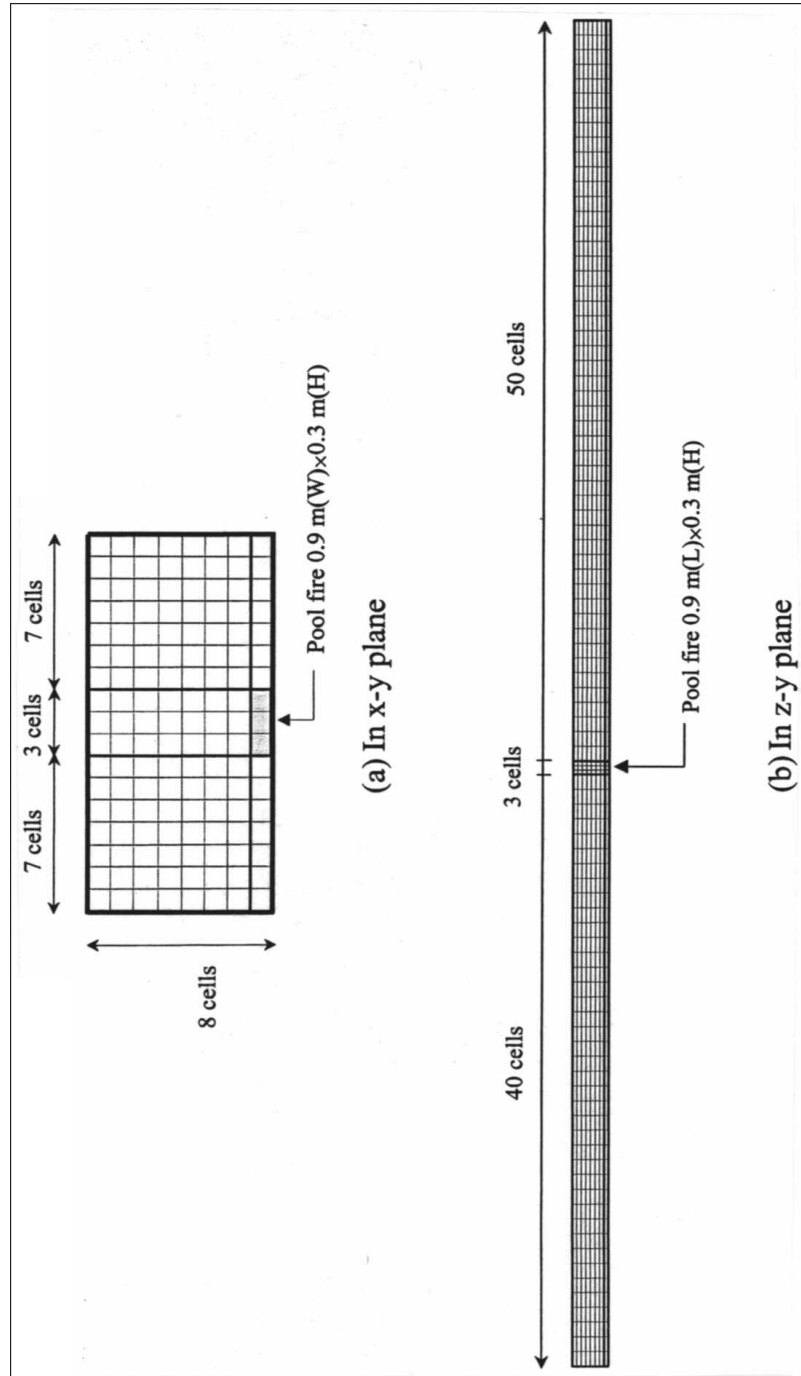


Figure 1. Configuration of tunnel pool fire experiment.

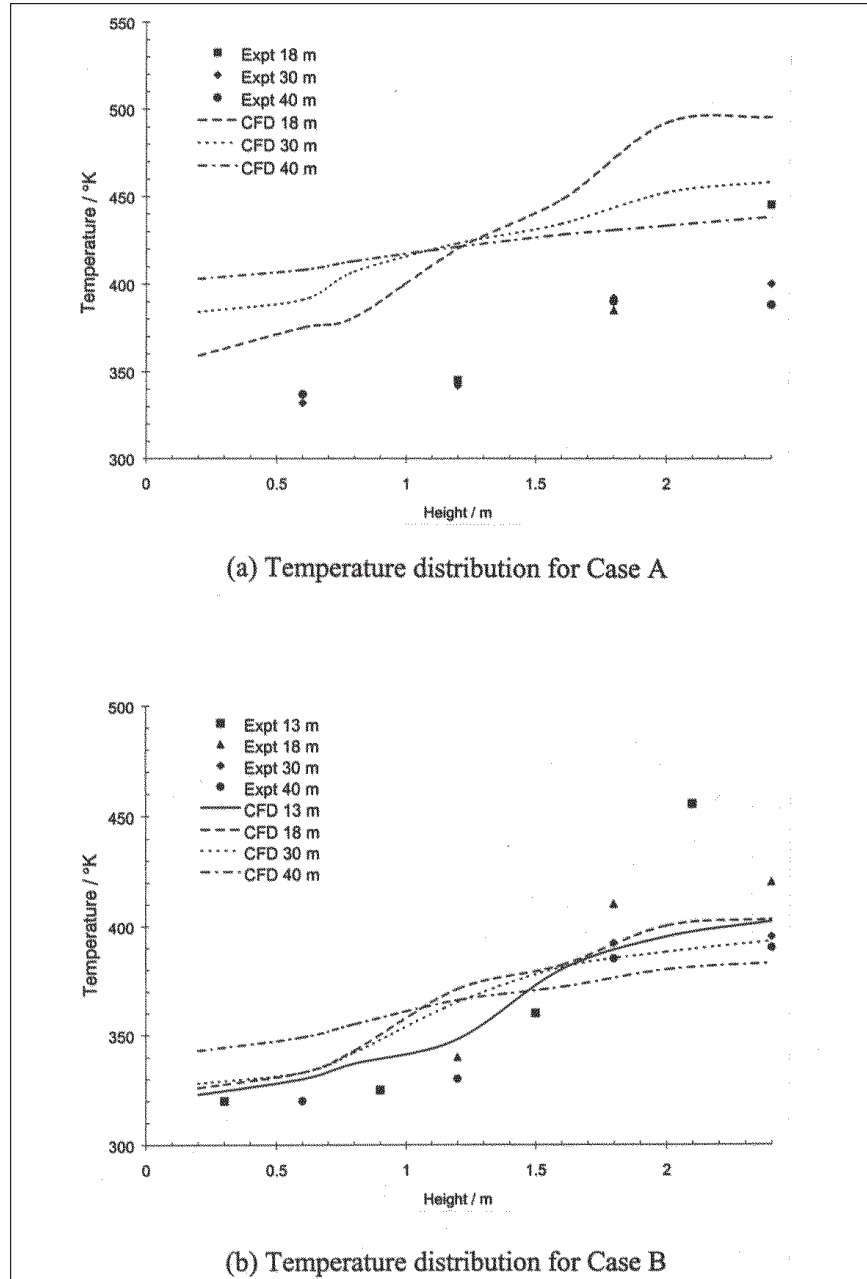


Figure 2. Experimental and predicted vertical temperature profiles downstream of the fire without taking account of radiation losses.

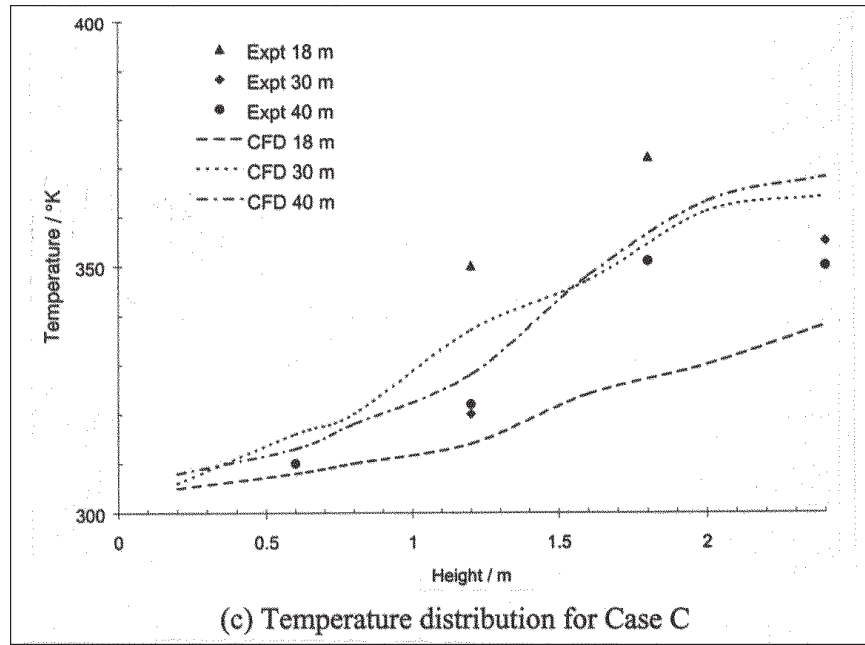


Figure 2. (Cont'd.)

### Case A—Ventilation Air Speed of $0.5 \text{ ms}^{-1}$

The temperature distributions for case A, which corresponds to a low ventilation rate, are shown in Figure 2(a). It can be seen that although the shape of the temperature profiles generally matched with the experimental data, the predicted values are about  $120^\circ\text{K}$  higher. Vertical stratification is observed at 18 m downstream of the fire as a hot upper smoke layer was formed at 1.5 m above the ground. Smoke was not extracted; while it was blown to one direction by the longitudinal ventilation air flow, the whole cross-section downstream of the fire would be filled with hot smoke and gas. The temperature profiles at 30 m and 40 m are getting flat, which indicate that smoke stratification was gradually lost downstream of the fire.

Results of simulation on case A with radiation losses are presented in Figure 3(a). Note that the predicted temperatures decreased in comparison with Figure 2(a). It is clear from the figure that the simulation reproduced the general features of the plots. Although the predicted values are again higher, differences with the experimental results are smaller. The predicted values are about  $60^\circ\text{K}$  higher in average.

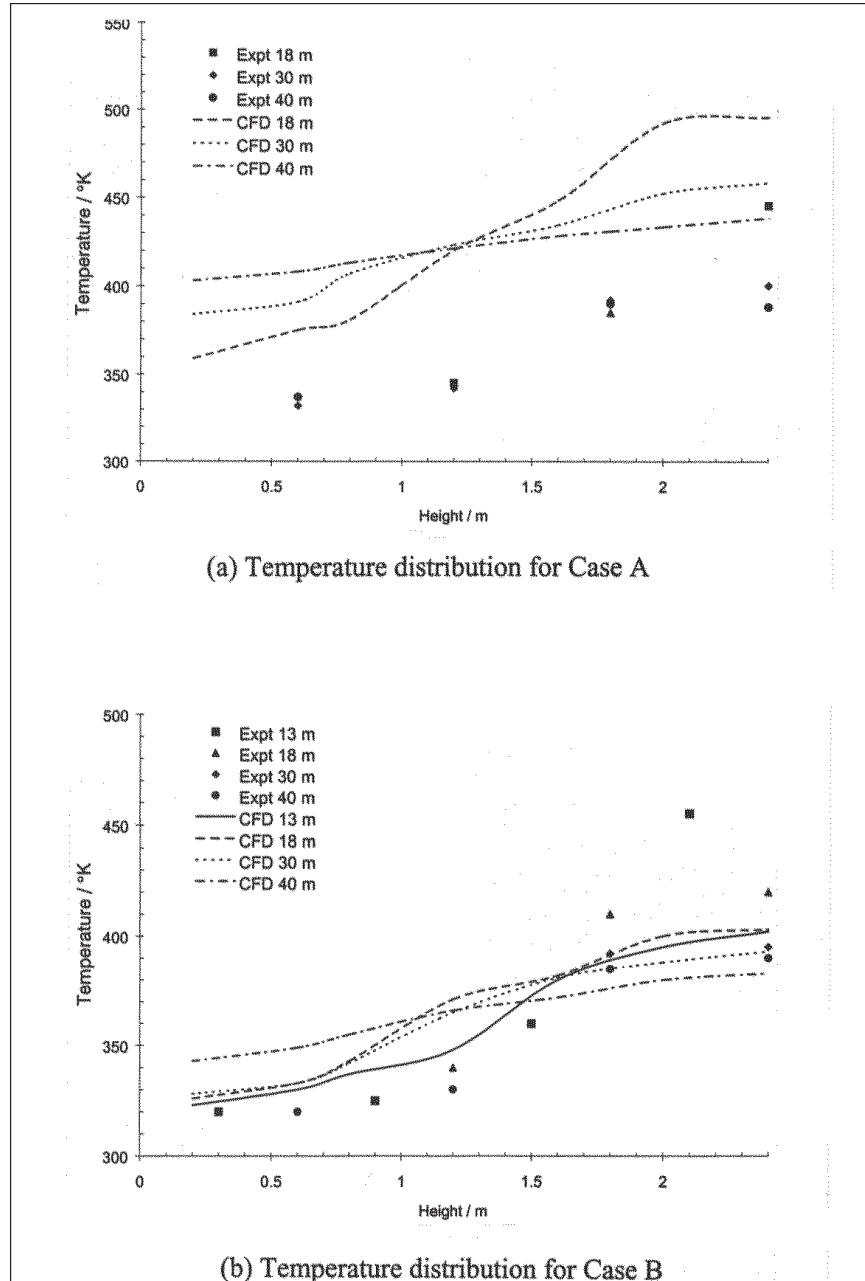


Figure 3. Experimental and predicted vertical temperature profiles downstream of the fire taking account of radiation losses.

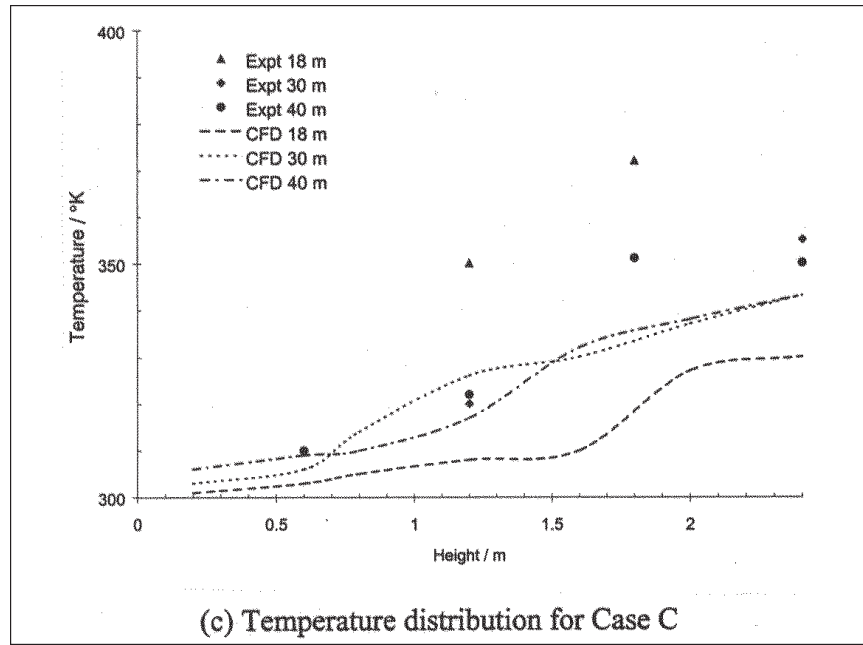


Figure 3. (Cont'd.)

### Case B—Ventilation Air Speed of $0.85 \text{ ms}^{-1}$

Simulation results for case B of medium ventilation rate are shown in Figures 2(b) and 3(b). More experimental data on the smoke layer for case B are provided to perform a more detailed comparison. The shapes of the temperature profiles agreed reasonably well with the experimental data. In general, the upper-layer gas temperatures were predicted to within  $50^\circ\text{K}$  with a general trend toward over-prediction of the temperatures, except at 18 m downstream of the fire (under-predicted by  $10^\circ\text{K}$ ). Results for upper-layer temperatures agreed better with experiment than those for lower-layer temperatures.

Similarly, taking into consideration the radiation losses, the predicted temperatures as shown in Figure 3(b) became lower. The agreement level is comparatively better than the predictions that do not take account of radiation losses. The temperatures were predicted to within  $20^\circ\text{K}$ . In general, lower layer temperatures were over-predicted and upper layer temperature under-predicted, especially at 13 m downstream of the fire, where the predicted temperature is  $60^\circ\text{K}$  lower than the experimental data. The hot smoke layer was stratified at about 1.5 m above the ground as shown in Figures 2(b) and 3(b).

### Case C—Ventilation Air Speed of 2 ms<sup>-1</sup>

Temperature distributions for case C, corresponding to high ventilation rates, are shown in Figures 2(c) and 3(c). As shown in Figure 2(c), only temperature predictions downstream of the fire generally agree with the experimental data with a trend of over-prediction. The discrepancy was limited to 15°K. However, the discrepancy was enlarged to about 40°K for prediction at 18 m downstream of the fire. The accuracy of the predicted values in this near fire region is questionable, as the overall vertical temperatures are lower than those downstream of the fire by 30°K.

A comparison of temperature profiles taking radiation losses into consideration is shown in Figure 3(c). It can be seen that the simulation under-predicted the vertical temperature at various locations downstream of the fire. Although the experimental data at 18 m and 30 m are sparse, it appears that the model has under-predicted the vertical temperature. The deviation became more obvious for upper layer temperature prediction. Moreover, due to high ventilation air flow, the stratification effect downstream of the fire was almost damped out, as seen in both Figures 2(c) and 3(c).

## 4. COMPARISON OF THE FLAME SHAPE

In the tunnel pool fire experiment, the angle of flame with respect to the vertical was measured by taking pictures in a direction perpendicular to the flow. Air temperatures predicted in the region of the flame for the three cases are shown in Figures 4 and 5. The flames were deflected by longitudinal air flow as expected, and the deflection angle  $\theta$  depends on the air flow velocity as [14]:

$$\sin \theta = \begin{cases} 1 & \text{for } V' < 1 \\ (V') & \text{for } V' > 1 \end{cases} \quad (1)$$

$V'$  is expressed in terms of the dimensionless wind speed  $V$  through the specific heat of air at constant pressure  $C_p$  (1.0056 kJkg<sup>-1</sup>C<sup>-1</sup>); temperature of ambient air  $T_\infty$  (20°C); density of ambient air  $\rho_\infty$  (1.2 kgm<sup>-3</sup>); the density of fuel vapor  $\rho_f$  (4.73 kgm<sup>-3</sup>); and the heat of combustion  $\Delta H_c$  (44.4 × 10<sup>3</sup> kJkg<sup>-1</sup>):

$$V' = V \left( \frac{2C_p T_\infty \rho_\infty}{\pi \rho_f \Delta H_c} \right)^{-1/3} \quad (2)$$

$V$  is given by the actual wind speed  $v$  and the characteristic plume velocity  $u$  as:

$$V = \frac{v}{u} \quad (3)$$

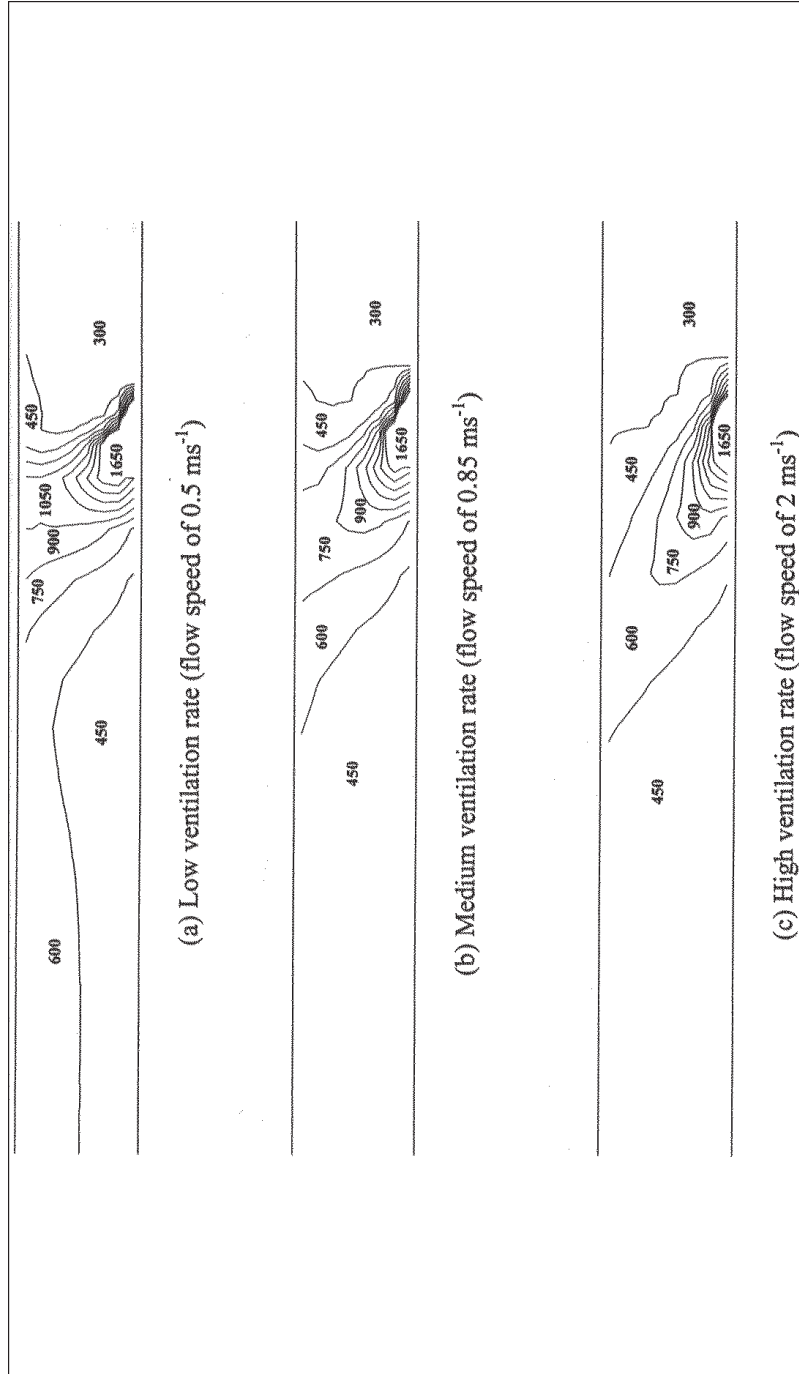


Figure 4. Predicted flame shape and temperature (K) without taking account of radiation losses.

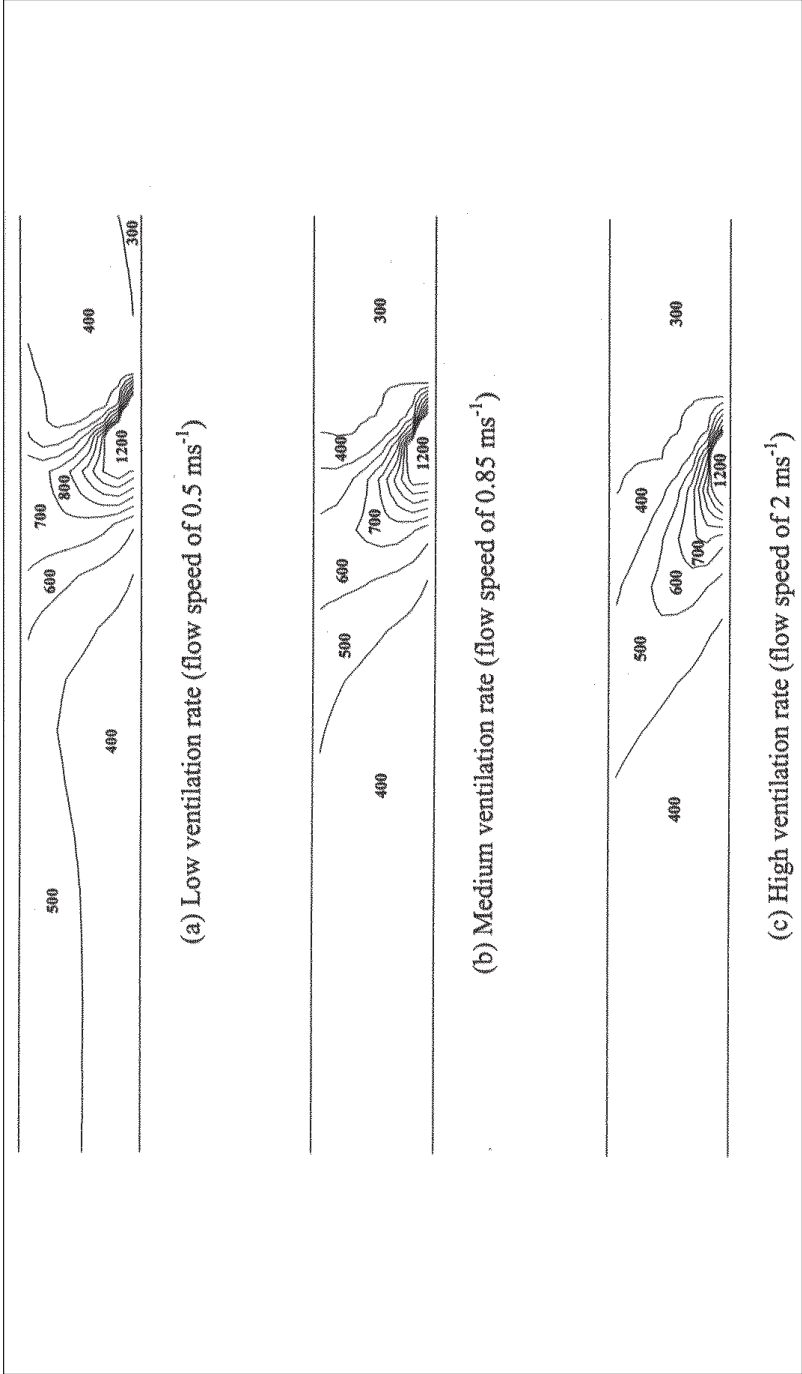


Figure 5. Predicted flame shape and temperature (K) taking account of radiation losses.

with  $u$  expressed in terms of the heat release of fire  $Q$  in kW:

$$u = 1.9 Q^{1/5} \quad (4)$$

The calculated deflection angles of flames corresponding to CFD computations are shown in Table 3, together with experimental measured values and  $\theta$  calculated from equation (1). It is found from the simulations that a cross-flow velocity of only  $0.5 \text{ ms}^{-1}$  was sufficient to deflect the flame significantly, although the flame appeared to be relatively insensitive to the difference in fire size.

## 5. DISCUSSION

In comparing numerical results with the pool fire experiments in a tunnel, several points are observed concerning the following factors.

### Air Flow Pattern and Stratification

A plume induced by a thermal object would rise due to buoyancy. Upon reaching the ceiling, the plume would be deflected radially outward to form a ceiling jet. For tunnel pool fires, the radial plume would be deflected at the sidewalls of the tunnel, giving one-dimensional movement against the external ventilation flow.

The traveling speed of smoke would decrease gradually due to cooling by entrained air with loss of buoyancy. Simulation results for cases A and B demonstrated that hot air would be stratified in regions from 30 m to 40 m. Without a smoke exhaust system, smoke would be cooled down and trapped when mixing with the counter-flowing air some distance away from the fire.

Table 3. Measured and Predicted Flame Angles in Tunnel Pool Fire Experiment

Case	Heat release rate (MW)	Air flow speed ( $\text{ms}^{-1}$ )	Angle of flame tilted to vertical during steady state (Deg.)		
			Measured	CFD	Calculated by Equation (1)
A	2.44	0.5	54	23	30
	1.65		—		33
B	0.065	0.85	59	45	49
	2.27		—		51
C	0.058	2	66	64	65
	2.02		—		66

Stratification was not noticeable in case C due to the high longitudinal ventilation air flow applied. The air flow was strong enough to blow hot air downstream.

### **Effect of Wind Velocity and Heat Release Rate**

Increasing the longitudinal ventilation velocity would increase the rate of transport of hot air downstream. As shown in the simulations, a large quantity of hot air would be blown to the other end of the tunnel when the longitudinal air speed is increased. The flow would be accelerated due to obstruction by the plume.

The measured temperature decreased with the increase in wind velocity. A possible explanation is the shifting of the plume to downstream as the size of the burning surface reduced [15], reducing the buoyancy head responsible for the upstream flows. The stronger the wind, the more pronounced this shift becomes, and the smaller the size of the burning surface.

Another reason for the decrease in measured temperature is that the pool fire was small in size and fuel-controlled. Additional air supplied by operating the ventilation system would not be involved in the combustion. This would even give a cooling effect on the fuel and the tunnel environment. The assumption of taking the heat release rate of the fire as constant in the simulations affects the energy distribution inside the tunnel volume. Experience shows that the temperatures predicted agreed well with experiments except for locations very near to the fire [16]. On the contrary, large pool fires ( $\sim 100 \text{ m}^2$ ) in tunnels are likely to be ventilation-controlled. Any additional ventilation will increase the heat release rate of the fire [17].

As a result, ventilation strategies to maximize fire safety should be determined carefully. This applies especially to accidents with large fuel spillage. Ventilation should be kept to a minimum for such vehicle fires.

### **Radiation Flux**

The total heat flux is the sum of the radiation flux from the soot and gases, mainly  $\text{CO}_2$  and  $\text{H}_2\text{O}$ , and the convective heat flux. The radiative heat transfer to the walls depends on the temperature of the wall and smoke and the emissivity of the smoke. Experiments demonstrated that the temperature would increase with height, because of the growth of flame and the hot gas layer, especially for locations near the fire source [18]. Since the increasing mass transfer would cause more blockage to convective transfer, the convective heat flux would decrease slightly with height, while radiation becomes the dominant heat transfer mechanism at high locations.

However, it is difficult to model thermal radiation in fire simulations without using a separate radiation model linked up with the fluid flow calculation. Radiative heat transfer was not modeled in the simulations. The proportion of heat released in the flame transferred by radiation to the total heat output varies

considerably for different fuels and sizes of fuel pan, but mostly falls within the range of 1/5 to 2/5. There was no drastic change in the profile of predicted temperature curves after the radiation fraction was taken out, but the deviations between experimental and predicted values are generally narrowed. The nearest thermocouple was placed at 13 m from the fire, such that the effect of radiative heat flux at thermocouples can be neglected [19].

### **Combustion Models in Tunnel Fire Simulation**

During the tunnel pool fire experiment, the fuel reacts with longitudinal air flow to form products of combustion, smoke, and various gases. The smoke production rate after operating the longitudinal ventilation system is much higher than for a natural ventilation fire [20], so the smoke concentration would increase quite significantly in the downstream area. The unburned gases from the fire might spread until they mix with sufficient oxygen for complete combustion. The combustion products are usually formed in a series of chemical reactions. In order to accurately know the reaction kinetics and combustion rate in tunnel fires, a combustion sub-model might be included in the computational algorithm. However, experimental measurement and field modeling studies on smoke distribution are inadequate. Different combustion models are examined in enclosure fire simulation, including a small-scale tunnel fire experiment in the laboratory [21]. The study indicates that current turbulent combustion models are inadequate to account for the interaction of combustion, turbulence, and radiative heat transfer of participating media including smoke and soot.

## **6. CONCLUSION**

By comparing CFD predictions with full-scale testing data on tunnel pool fire, fire field models are suitable for predicting the environment in a tunnel due to an accidental fire. This technique can be applied in designing safety ventilation systems and the associated environmental control systems in tunnels. It is well demonstrated that this kind of CFD software would give reasonably accurate predictions of vertical temperature profiles along the tunnel axis. Roles played by the environmental control system, such as operating the longitudinal ventilation system, can be clearly visualized.

Active updating of the CFD technique is important for fire safety engineering design. A key need is to develop better models of turbulence with intermediate chemical kinetics. The general acceptance of such models as a practical tool for safety and environmental control systems design and assessment would require more systematic efforts to validate them. This will depend on the establishment of a coherent database of test data. In the event, radiation losses, heat release rate estimates, selection of input data, judgment, and the evaluation of the predicted results should be watched carefully in CFD simulation.

## REFERENCES

1. S. Kumar, N. Hoffmann, and G. Cox, Some Validation of JASMINE for Fires in Hospital Wards, in lecture notes in engineering on *Numerical Simulation of Fluid Flow and Heat/Mass Transfer Processes*, Springer-Verlag, New York, pp. 159-169, 1986.
2. R. N. Mawhinney, E. R. Galea, N. Hoffmann, and M. K. Patel, A Critical Comparison of a PHOENICS Based Fire Field Model with Experimental Compartment Fire Data, *Journal of Fire Protection Engineering*, 6, pp. 137-152, 1994.
3. A. N. Beard, Fire Models and Design, *Fire Safety Journal*, 28, pp. 117-138, 1997.
4. A. J. Grandison, E. R. Galea, and M. K. Patel, Fire Modelling Standards/Benchmark Report on Phase 1 Simulations, *Paper No. 01/IM/72*, CMS Press, 2001.
5. A. J. Grandison, E. R. Galea, and M. K. Patel, Fire Modelling Standards/Benchmark Report on Phase 2 Simulations, *Paper No. 01/IM/81*, CMS Press, 2001.
6. V. B. Apte, A. R. Green, and J. H. Kent, Pool Fire Plume Flow in a Large-Scale Wind Tunnel, *Fire Safety Science Proceedings of the Third International Symposium*, pp. 425-434, 1991.
7. PHOENICS Version 3.2, *Concentration, Heat and Mass*, CHAM Co., London, United Kingdom, 1999.
8. D. F. Fletcher, J. H. Kent, V. B. Apte, and A. R. Green, Numerical Simulations of Smoke Movement from a Pool Fire in a Ventilated Tunnel, *Fire Safety Journal*, 23, pp. 305-325, 1994.
9. H. Koseki and H. Hayasaka, Estimation of Thermal Balance in Heptane Pool Fire, *Journal of Fire Science*, 7, pp. 237-250, 1989.
10. N. C. Markatos, M. R. Malin, and G. Cox, Mathematical Modelling of Buoyancy-Induced Smoke Flow in Enclosure, *International Journal of Heat and Mass Transfer*, 25, pp. 63-75, 1982.
11. O. Megret, and O. Vauquelin, A Model to Evaluate Tunnel Fire Characteristics, *Fire Safety Journal*, 34, pp. 393-401, 2000.
12. G. Cox and R. Chitty, A Study of the Deterministic Properties of Unbounded Fire Plumes, *Combustion and Flame*, 39, pp. 191-209, 1980.
13. K. S. Mudan, Thermal Radiation Hazards from Hydrocarbon Pool Fires, *Progress in Energy and Combustion Science*, 10, pp. 59-80, 1980.
14. P. K. Raj, K. S. Mudan, and A. N. Moussa, Experiments Involving Pool and Vapour Fires from Spills of LNG on Water, *Report no. CG-D-55-79, NTIS AD77073*, U.S. Coast Guard, Washington, D.C., 1979.
15. J. Brandeis and D. J. Bergmann, A Numerical Study of Tunnel Fires, *Combustion Science and Technology*, 35, pp. 133-155, 1983.
16. Permanent International Association of Road Congress (PIARC). Study Methods. *Fire and Smoke Control in Road Tunnels*, Chapter IV, 1999.
17. R. O. Carvel, A. N. Beard, and P. W. Jowitt, The Influence of Longitudinal Ventilation Systems on Fires in Tunnels, *Tunnelling and Underground Space Technology*, 16, pp. 3-21, 2001.
18. Z. Yan and G. Holmstedt, CFD Simulation of Upward Flame Spread Over Fuel Surface, *Proceedings of the 5th International Symposium on Fire Safety Science*, IAFFS Conference, pp. 345-356, 1997.
19. P. J. Woodburn and R. E. Britter, CFD Simulations of a Tunnel Fire—Part I, *Fire Safety Journal*, 26, pp. 35-90, 1996.

20. W. K. Chow, On Smoke Control for Tunnels by Longitudinal Ventilation, *Tunnelling and Underground Space Technology*, 13, pp. 271-275, 1998.
21. H. Xue, J. C. Ho, and Y. M. Cheng, Comparison of Different Combustion Models in Enclosure Fire Simulation, *Fire Safety Journal*, 36, pp. 37-54, 2001.

Direct reprint requests to:

Jojo S. M. Li  
Department of Building Services Engineering  
The Hong Kong Polytechnic University  
Hong Kong, China  
e-mail: jojo.li@arup.com